Minerals Engineering 116 (2018) 152–162

Contents lists available at ScienceDirect

Minerals Engineering

journal homepage: www.elsevier.com/locate/mineng

Grade and product quality control by microCT scanning of the world class Namakwa Sands Ti-Zr placer deposit West Coast, South Africa: An orientation study

A. Rozendaal[a,*], S.G. Le Roux[b], A. du Plessis[b], C. Philander[a,1]

[a] Department of Earth Sciences, University of Stellenbosch, South Africa
[b] CAF X-ray Facility, University of Stellenbosch, South Africa

ARTICLE INFO

Keywords:
Namakwa Sands
Ti-Zr heavy minerals
MicroCT scanning

ABSTRACT

The Namakwa Sands operation is a world class producer of zircon, rutile and ilmenite from mainly semi-consolidated marine and dune sands. This orientation study shows that the high density contrast between the economic minerals as well as the diverse gangue mineralogy allows the use of microCT scanning as a qualitative and quantitative analytical tool. The method has demonstrated the ability to quantify final product quality, grain size distribution, grain shape definition and the identification of external and internal mineral textures. Grain size distribution data generated by microCT scans compares well with data produced by other analytical methods. As a result, the method has the potential to be applied to in situ resource calculations (total heavy minerals - THM, valuable heavy minerals - VHM), run-of-mine (ROM) grade control and the various stages of the mineral beneficiation process. MicroCT scanning applied to heavy mineral producing operations appears promising and should be further assessed against traditional analytical methods. The method also has the ability to assist sedimentological studies with respect to in situ quantitative grain size and sphericity determinations.

1. Introduction

The Namakwa Sands heavy mineral placer deposit is located near Brand-se-baai some 300 km north of Cape Town, along the West Coast of South Africa. Tronox Limited controls the operation, which has developed into a significant, global producer of titanium slag, pig iron, ceramics quality zircon and rutile concentrates (Fig. 1). The deposit is classified as a mega-resource with 1.17 billion tons of in-situ ore, containing an estimated 92.6 Mt of total heavy minerals and the equivalent of 23.9 Mt TiO_2 units and 9.4 Mt zircon (Jones, 2009; Philander and Rozendaal, 2015a). Currently, mechanized dry mining of mostly semi-consolidated sand takes place in several open pits, allowing an annual production capacity of 23 Mt run-of-mine. Mineral processing capacity has the ability to deliver 450 kt ilmenite as well as 110 kt zircon and 25 kt rutile annually. The ilmenite is supplied to their titanium smelter at Saldanha Bay, producing at least 180 kt of titanium slag and 120 kt of pig iron per year (Philander and Rozendaal, 2015a).

2. Geological background

The ore mineral suite is associated with Early Pliocene (~5 Ma) to the Late Pleistocene siliciclastic, arenaceous sediments and hosted by two adjacent ore bodies referred to as Graauwduinen West (GD West) and Graauwduinen East (GD East; Fig. 2). GD West consists of three strandline-dune couplets set in a transitional shallow marine-aeolian environment, whereas GD East comprises a largely unrelated dune deposit. Superimposed onto the ore-bearing sequence is a pseudo-stratigraphy of duricrust that effectively cemented the bulk of the mineralized sands to various degrees of hardness. The two ore bodies contrast in their bulk chemistry and mineralogy. GD West features noticeable better total heavy mineral grades, accompanied by conspicuously high proportions of the gangue minerals garnet and pyroxene.

The valuable mineral fraction (VHM) is predominated by ilmenite ($FeTiO_3$), followed in abundance by leucoxene (an alteration product of ilmenite), zircon ($ZrSiO_4$) and rutile (TiO_2). Their geochemistry, mineralogy and petrography are variable, but the bulk of the current valuable mineral fraction is recoverable to premium-grade products. The proximal, Mesoproterozoic Namaqualand Metamorphic Province is considered the main contributor to the current heavy mineral population via established fluvial-marine courses and a fluvial-aeolian corridor (Philander and Rozendaal, 2015a, 2015b; Rozendaal et al., 2017).

* Corresponding author.
E-mail address: ar@sun.ac.za (A. Rozendaal).
[1] Present address: Tronox Namakwa Sands, South Africa.

http://dx.doi.org/10.1016/j.mineng.2017.09.001
Received 6 June 2017; Received in revised form 22 August 2017; Accepted 14 September 2017
Available online 29 September 2017
0892-6875/

Fig. 1. Locality of the various operations associated with the mining and beneficiation of the Namakwa Sands heavy mineral deposit along the West Coast of South Africa.

3. Minerals processing

The production of saleable minerals from a heavy mineral deposit requires the physical separation of individual mineral grains. Throughout the text, grains refer to individual sand grains on mm scale. Separation is accomplished by exploiting differences in four mineral characteristics: density, grain size, magnetic susceptibility and electrical conductivity. The complexity of the ore characteristics observed at Namakwa Sands, translates into a challenging and variable processing response. Only mineral grade, liberation, magnetic deportment, grain size and grain chemistry are considered as meaningful mineral recovery drivers (Philander and Rozendaal, 2014). The successful mineral beneficiation process at Namakwa Sands is performed at four different plants as demonstrated by the flow chart in Fig. 3.

- Primary concentration (PCP) by wet spiral separation of the −1 mm +45 μm screened fractions takes place at two plants proximate to the mine face. The total heavy mineral concentration (THM) of the run-of-mine feed is increased tenfold by this process. Duricrust cemented oversize feed is reduced by autogenous milling.
- Secondary concentration (SCP) occurs at a centralised plant at the mine site. Low Intensity Magnetic Separators (LIMS) remove highly magnetic material (essentially magnetite) from a PCP East and PCP West concentrate blend. In a next phase, Wet High Intensity Magnetic Separators (WHIMS) separate the resultant non-magnetic material in a magnetic fraction, containing mainly ilmenite and garnet and a non-magnetic fraction comprising zircon, rutile, leucoxene and low-density gangue. Further WHIMS treatment of the magnetic fraction produces a Magnetic Concentrate, whereas a wet gravity section upgrades the non-magnetic fraction to produce a Non-magnetic Concentrate. Both the SCP concentrates are attritioned to remove siliceous surface coatings.
- Final mineral beneficiation is achieved at the MSP (mineral separation plant; Fig. 3). The two different SCP concentrates are processed in two different circuits, namely the Magnetic Circuit and Non-magnetic Circuit to produce the ilmenite, zircon and rutile products. The Magnetic Circuit employs drum magnetic separators, followed by High Tension Roll (HTR) electrostatic separators to reject garnets and other silicates to produce the ilmenite product. The Non-magnetic Circuit consists of four sub-circuits. The non-magnetic concentrate is upgraded by Induced Roll Magnetic Separators (IRMS) by rejecting the moderately to strongly magnetic minerals. Hepworth Acid Leaching (HAL) is used to remove mineral surface coatings, which suppress electrostatic separation and is followed by mechanical attritioning. In a following stage, the Wet Gravity Circuit removes low-density gangue to produce a high-grade primary concentrate, and a secondary lower grade concentrate. Final separation takes place in the Dry Mill Circuit that houses a combination of multiple stages of electrostatic and magnetic separators to produce a prime grade zircon and lower quality zircon product (Zirkwa™) and a prime rutile and lower quality Tiokwa™ product (Fig. 4). The final ilmenite, zircon and rutile products are railed to Saldanha Bay, where the ilmenite is smelted, whilst the zircon and rutile are stored prior to export shipping (Fig. 1).

4. Aims and objectives

To ensure the reliability of in situ resource estimates, grade of run-of-mine plant feed, effectiveness and efficiency of the various stages during the mineral separation process and quality control of the final products, the mine employs a diversity of analytical methods. THM content is determined by heavy liquid separation. Optical microscopy-assisted mineral point counting is used to identify and quantify mineral phases during various stages of the resource estimate, mining and mineral separation. Sieve analyses (mechanical screening) to determine grain size distribution is commonly used. XRF quantifies titanium and zirconium content as well as deleterious elements such as silica, iron, phosphorous, uranium and thorium from primary ore to final product. XRD is used for mineral phase identification and quantification. Scanning electron microscope (SEM) based methods such as Mineral Liberation Analyser (MLA) and QEMSCAN assist with mineral phase identification, mineral textures, gangue-mineral intergrowth relationships and their quantification as well as grain size distribution. The SEM is also used to study surface coatings of ore minerals. EMPA and LA-ICP-MS are methods used to identify both major and trace element chemistry of mineral phases and their inclusions or intergrowths.

Although some of the instrumentation for the more routine analytical methods are physically based on the mine and may have an approximate turnaround time of 24 h to deliver data, the more sophisticated off-site methods required significantly longer periods to generate results and effect implementation. The aim of this orientation study is to introduce and test a relatively new method, microCT (X-ray micro Computed Tomography) which allows differentiation between objects and minerals based on their density and in some cases trace element contrast (Ketcham and Carlson, 2001; Cnudde and Boone, 2013; Parian et al., 2015). Its use in minerals processing especially for granular minerals has been demonstrated initially by Miller and Lin (2004) and particle shape analysis demonstrated by Lin and Miller (2005) and Zhao and Wang (2015). It is considered in this case study that the method has the potential to provide valuable high resolution quantitative data in 3D relating to the heavy minerals industry. It can contribute towards phase identification, grain size and shape distribution as well as internal and external textural features of ore and gangue minerals. The data can be generated off site or potentially on site by a one-step, non-destructive process, which should be able to reduce turn-around time, improve overall productivity and production cost. This orientation study tested four samples from the mine, three of which are final

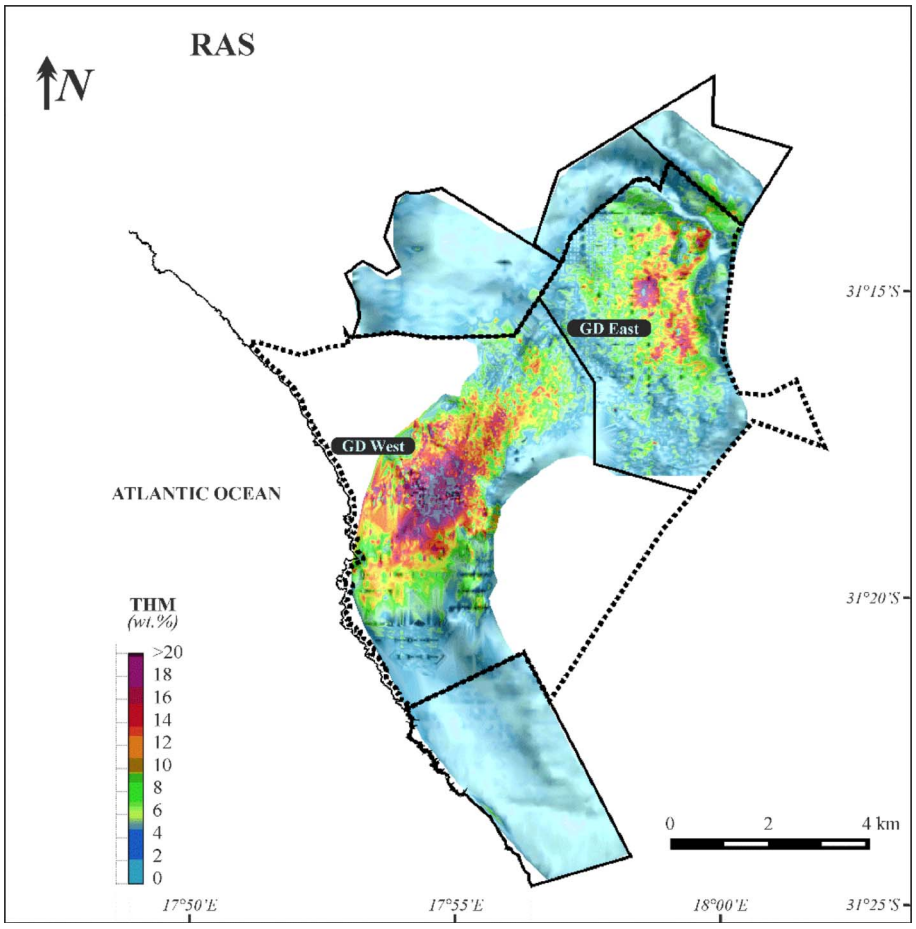

Fig. 2. Distribution and total heavy mineral grades (THM) of the extensive upper part (Red Aeolian Sands, RAS) of Namakwa Sands placer deposit along the West Coast of South Africa. (For interpretation of the references to colour in this figure legend, the reader is referred to the web version of this article.)

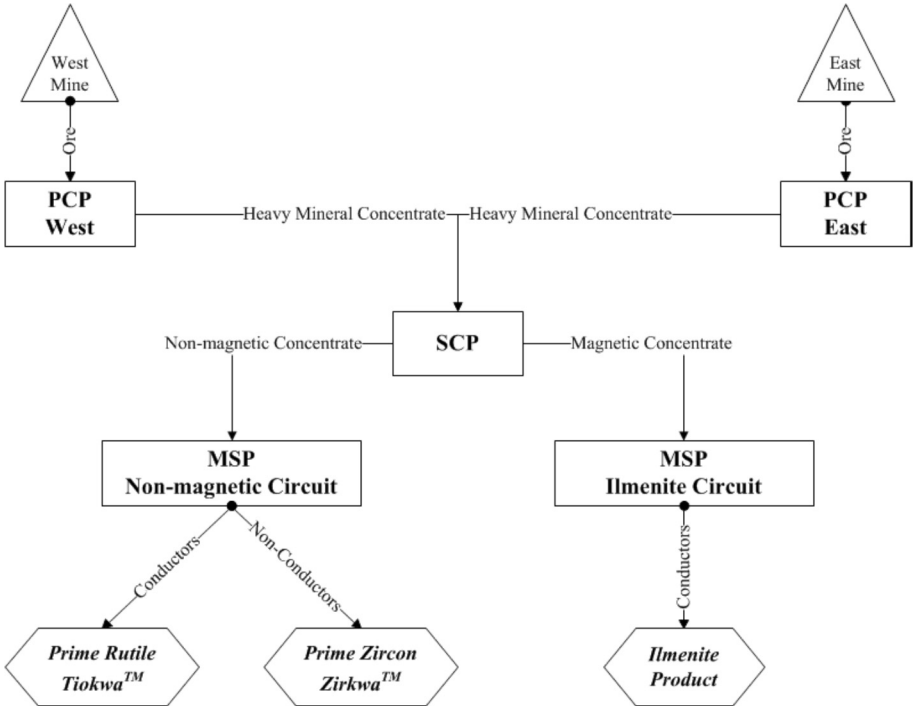

Fig. 3. Simplified process flow sheet used at Namakwa Sands mineral processing operation. (Philander and Rozendaal, 2014, 2016).

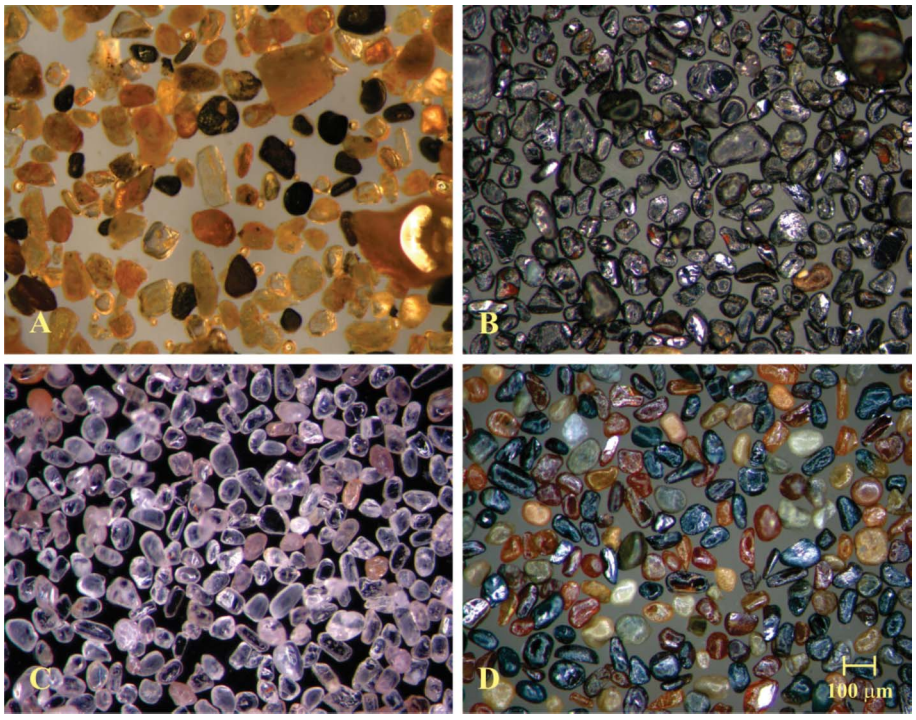

Fig. 4. Run-of-mine ore from the Namakwa Sands mine (A). Total heavy mineral content is approximately 10%. Ilmenite concentrate produced as feed stock for the titanium smelters in Saldanha Bay (B). Prime rutile concentrate (C) and prime zircon for the export market (D). (Optical microscopy, incident light, images taken at the same magnification).

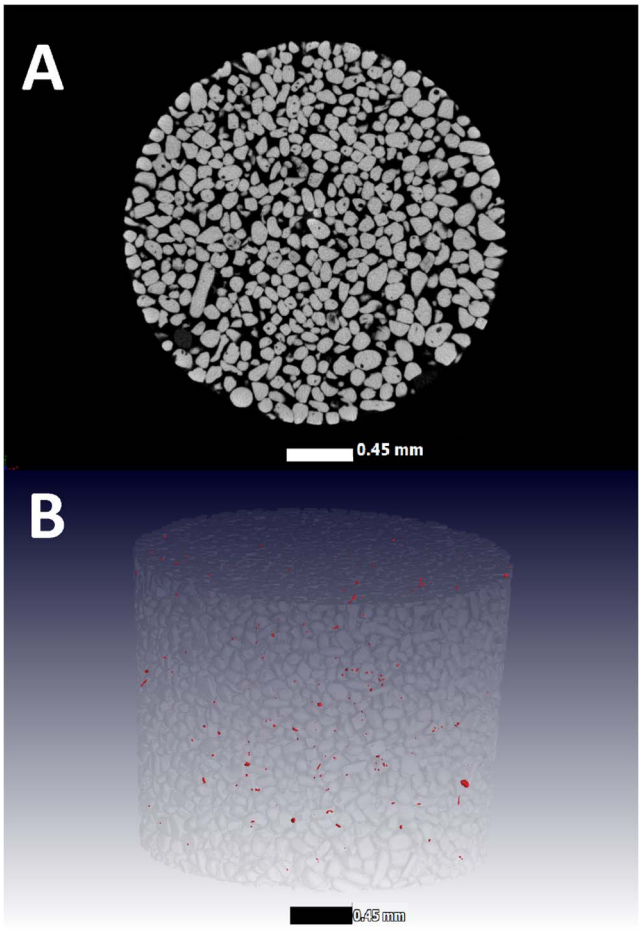

Fig. 5. (A) Prime zircon concentrates showing high quality and purity. Small dark spots are low density voids/regions consisting mainly of apatite and diverse fluid or gas. Contrast is enhanced to visualize zircon. (B) Three dimensional image showing distribution of fine, high density grains, confirmed as monazite, in the concentrate. MicroCT voxel size 1.5 µm, field of view 3 mm.

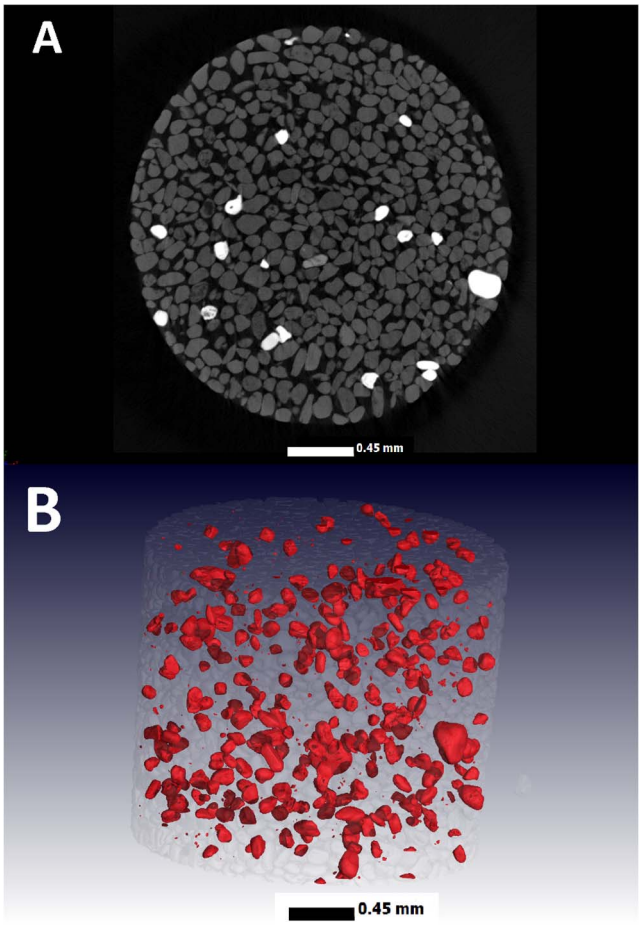

Fig. 6. Prime rutile concentrates with bright, high density grains of zircon (A). Contrast is enhanced to visualize rutile. The zircon distribution is accentuated by the 3D image. Mineral identification is confirmed by the elongated, tetragonal shape of the grains and SEM analyses (B). MicroCT voxel size 1.5 µm, field of view 3 mm.

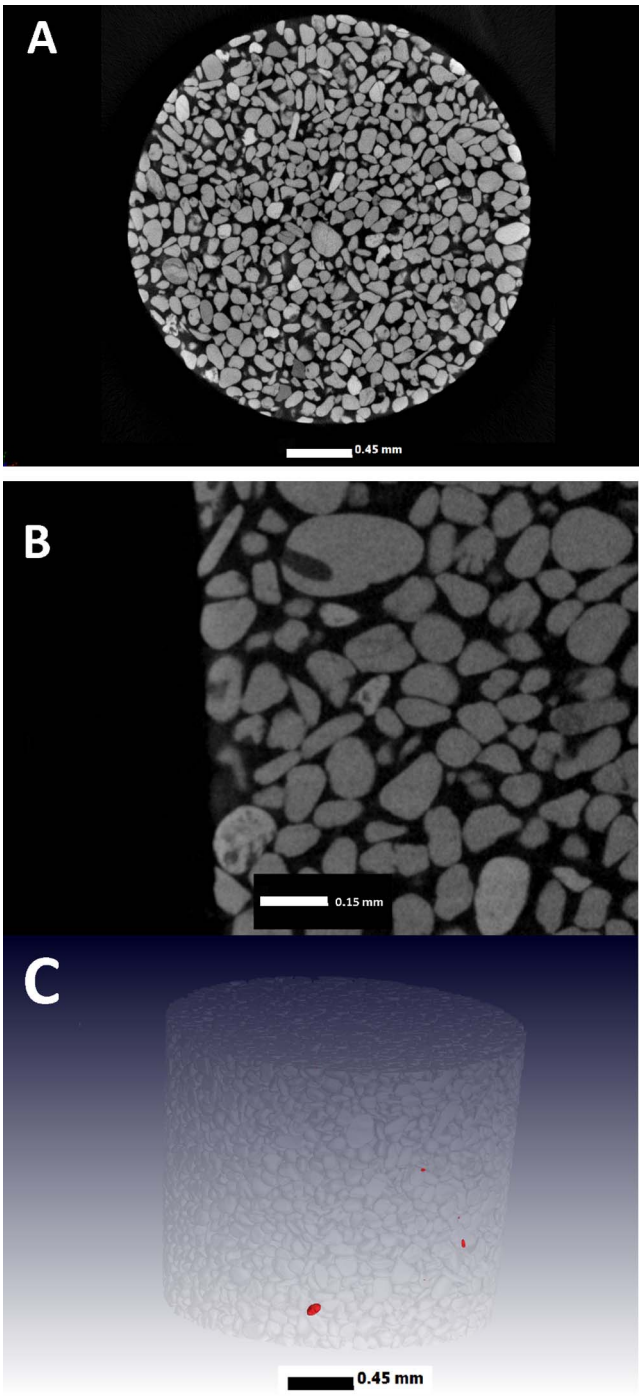

Fig. 7. Ilmenite concentrate consist of a diversity of grains with variable composition as indicated by the contrasting grey scale (A). Contrast is enhanced to visualize ilmenite. At high magnification the complex internal textures of ilmenite as well as low density inclusions are clearly visible (B). The concentrate also has scattered grains of zircon based on the elongate grain shape and SEM analyses (C). MicroCT voxel size 1.5 μm, field of view 3 mm. Magnified image field of view 1 mm.

products and one a PCP concentrate from the RAS part of the GD East ore body to demonstrate "proof of concept".

5. Methodology

Three of the four samples studied were randomly collected from the prime zircon product, prime rutile product and ilmenite product stock piles and one sample from the PCP East heavy mineral concentrate which serves as feedstock to the SCP (Fig. 3). Feed stock mineralogy is diverse consisting of the valuable heavy minerals (VHM) which include ilmenite, leucoxene, rutile and zircon as well as heavy minerals with no or little economic value. These fractions combined define the THM suite. Minerals with density of less than 2.9 g/cm^3 such as quartz and feldspar may also be present. The selected samples have been subjected to chemical (Namakwa Sands mine laboratories) and QEMSCAN analyses (Exxaro Laboratories, Pretoria) for comparative purposes with the MicroCT results. Sieve analyses also referred to as mechanical screening was done at Namakwa Sands mine laboratories following international protocols and controls.

Sample size was reduced by means of a riffler and micro splitters in order to obtain a representative sample for scanning. MicroCT scanning was performed at the Stellenbosch University CT facility which has been described in detail by du Plessis et al. (2016). In order to obtain best quality images at highest possible resolution, settings were selected to optimize quality rather than processing time, using methodology described in du Plessis et al. (2017). Shorter scanning and analysis times could be possible once the methodology has been streamlined for this particular application. Each sample was placed in a small tubular transparent container with dimensions 3 mm diameter and 7 mm depth. Once appropriate settings were selected ensuring good X-ray parameters, each sample was then scanned for a period of 120 min within a General Electric Phoenix Nanotom S scanner at 120 kV with a current of 80 uA at a resolution of 0.0015 mm (1.5 μm). The X-ray spot size was limited using the "mode 1″ option, ensuring the X-ray spot is kept below the voxel size selected. Stepwise rotation of the sample was performed in 3600 steps in a full rotation of the sample. At each step, the first image acquired was discarded to ensure no movement artefacts are present and the subsequent 3 images averaged to produce higher quality acquisition. Each individual image acquisition time was 500 ms. Detector shift was activated which allows reduced central rotation axis artefacts by moving the detector horizontally between step positions. Reconstruction was performed with system-supplied Datos reconstruction software using a moderate beam hardening correction factor.

Post processing of the data and advanced image analysis was performed with Volume Graphics VG Studio Max 3.0 software where the advanced surface determination function allowed the identification and quantification of high density grains and their volumes. In the advanced surface determination, the edge of each grain is accurately determined based on local optimization of the gradient between background and material in the 3D image data. The result allows not only images of the grains and their internal details, but also quantitative analyses such as grain size distribution, largest grain size, number of grains, number of inclusions and shape analysis.

The detailed methodology to calculate mineral phase concentrations and grain size distribution included the use of the volume analyser tool which makes it possible to calculate the volume of the original grains and high or low-density grains relative to the bulk grain volume. These volumes can be expressed as weight per cent by using the average density of each mineral's phase. In addition to the above relative concentrations, which has been applied and described for another application by le Roux et al. (2015), grain size analysis was performed using an advanced methodology as follows. The newly implemented "foam structure analysis" module of VG Studio Max 3.0, is meant for analysing foam structures i.e. large air voids connected to one another. In this case the analysis was run on material instead of background as the situation relates to sand grains in contact with each other. In this case each grain is identified as an individual entity, even though they are touching each other in the container. A simpler methodology which has been demonstrated by Rothleitner et al. (2016) and Zhao and Wang (2015) makes use of grain mounting in resin or glue to ensure they do not touch each other during microCT scanning, which makes the analysis simpler but with a much reduced number of grains. In our work grains are placed in a container "as-is" and digitally separated. The advantages are that a much larger number of grains are analysed in one scan, less bias is present in grain selection and simplicity of sample

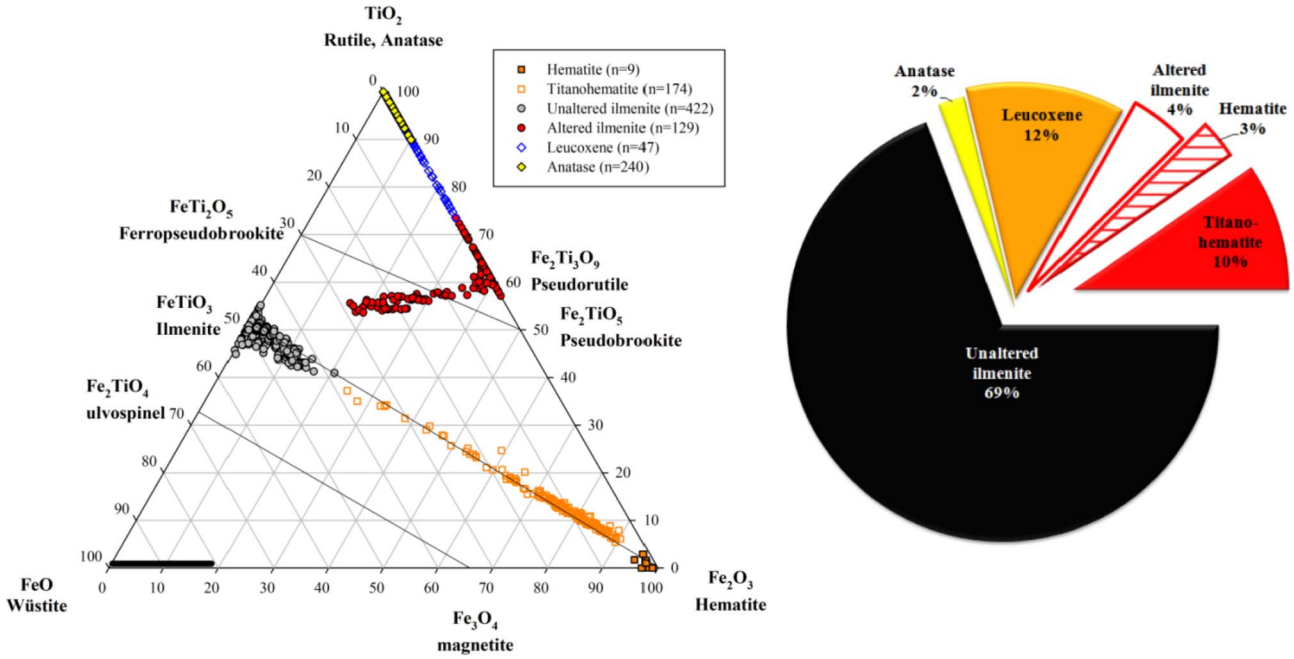

Fig. 8. Synoptic ternary diagram showing chemistry of titanium phases associated with the Namakwa Sands deposit. Ilmenite and rutile/anatase products are not homogeneous and display significant variation in chemical composition (Rozendaal et al., 2017).

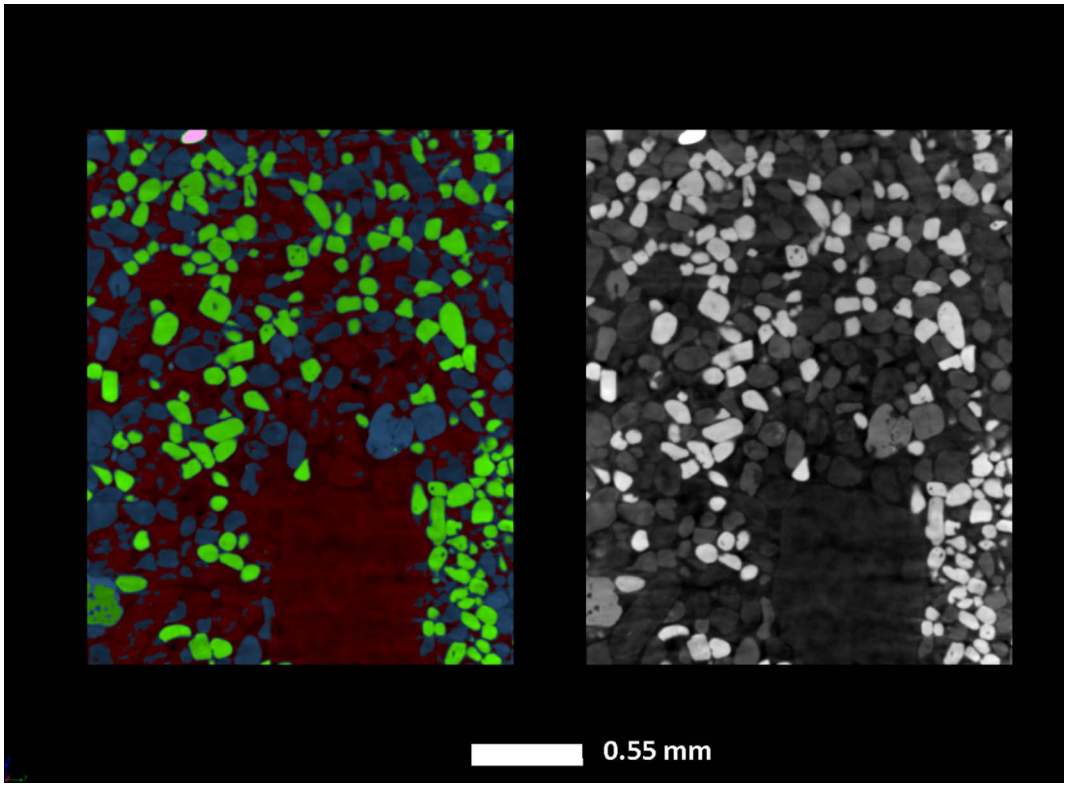

Fig. 9. CT images of the SCP feedstock which allowed the discrimination between the three dominant phases of the VHM fraction as well as accessory monazite. Grain size variation between the phases is clearly visible. Monazite – pink, zircon – green, ilmenite – blue and rutile – red. MicroCT voxel size 1.5 μm, field of view 3 mm. (For interpretation of the references to colour in this figure legend, the reader is referred to the web version of this article.)

preparation. The disadvantage could be potential errors in digital separation of grains, which could be assessed visually to ensure accuracy. This is also a time consuming analysis, requiring significant computing power. In both methods the grain volume, surface area, sphericity and other parameters are calculated for every individual grain and reported in a spreadsheet.

The final mineral product samples were used to standardize/calibrate the grey scale images against the mineral phase such as rutile, zircon and ilmenite. Grains of lower density were classified as gangue and those of higher density than zircon as minerals of potentially high radioactivity such as monazite.

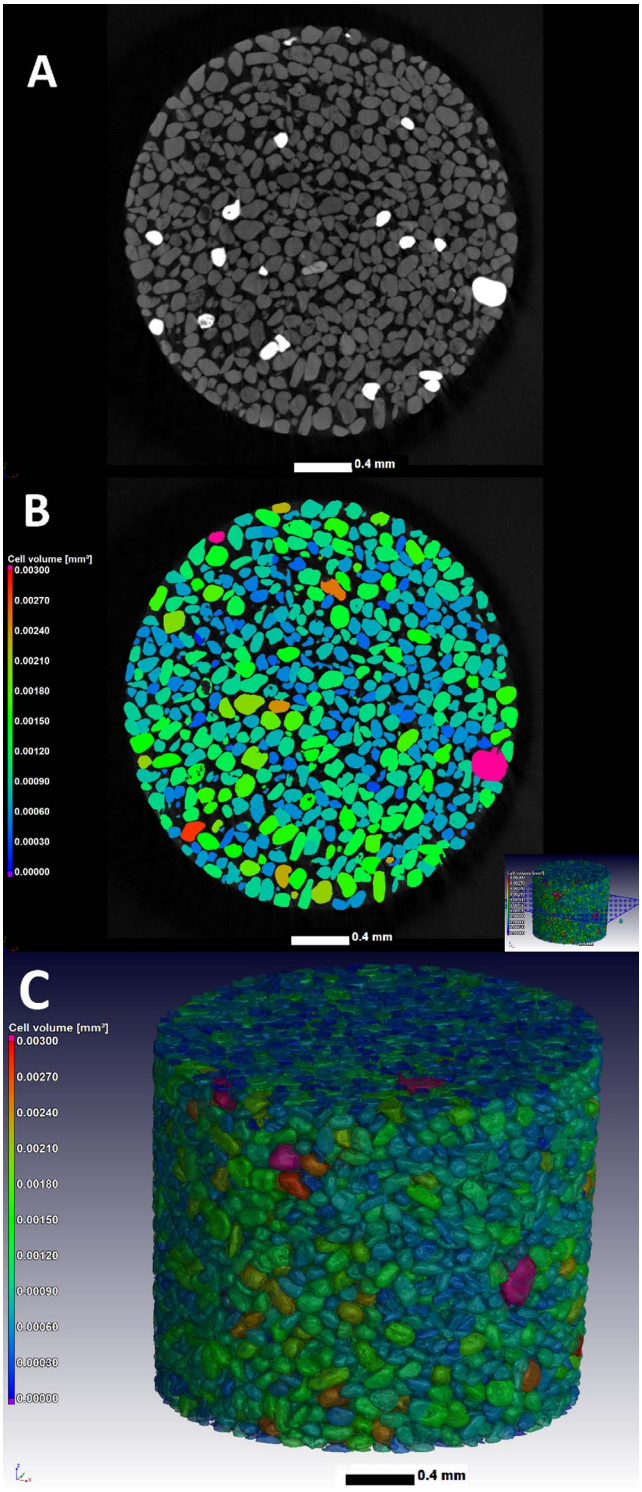

Fig. 10. (A) Prime rutile concentrate. (B) Colour coded volume analysis of rutile concentrate. (C) 3D image of colour coded volume analysis. MicroCT voxel size 1.5 μm, field of view 3 mm. (For interpretation of the references to colour in this figure legend, the reader is referred to the web version of this article.)

6. Results

6.1. Concentration

The microCT scan of the prime zircon concentrate shows an image (Fig. 5) consisting almost entirely of homogenous zircon grains with an occasional scattered high density grain, confirmed as monazite by SEM analyses. Low density gangue is effectively absent indicating good separation. The concentrate has 99.5% zircon content as calculated volumetrically and is confirmed by chemical and Qemscan analyses which indicate a 99.9% purity by weight. Previous work by Philander and Rozendaal (2014) on concentrates supports this result.

The prime rutile concentrate shows a fair abundance of high density grains confirmed as mainly zircon by SEM analyses (Fig. 6). Rutile grains are heterogeneous in composition as seen in Figs. 4C and 6 and this is confirmed by the subtle variation of grey scale in the microCT scans. Some of the grains are confirmed as leucoxene. Accessory grains of higher density confirmed as monazite, also occurs in the concentrate. The separation of rutile and zircon appears to be less effective and is demonstrated by the 97.2% by volume rutile content of the prime product. When analyzed by the QEMSCAN method the rutile concentrate has a 98.9% purity by weight when leucoxene is included in the calculation. This result suggests that some phases such as low titanium-high silica leucoxene were not included with the rutile population in the microCT scan.

The ilmenite concentrate contains minor scattered zircon grains (Fig. 7). The ilmenite grains are however heterogeneous as shown by variable shades of grey. Single grains show complex internal structures and host several inclusions many of which are apatite (Fig. 7B). This is a typical characteristic of ilmenite as demonstrated by Philander and Rozendaal (2015a) and Rozendaal et al. (2017) (Fig. 8). As a concentrate it has a volumetrically measured 99.9% ilmenite content. This high purity grade has been confirmed by chemical and Qemscan analyses and previous work (Philander and Rozendaal, 2014). Grain size is variable compared to the uniform size distribution of the zircon and rutile concentrates and is a function of variable chemistry and consequently density.

The SCP feedstock from the GD East part of the mine is a heavy mineral concentrate consisting of the VHM fraction and minor non-economic minerals. The microCT scan was able to distinguish the three dominant phases zircon, rutile and ilmenite (Fig. 9). Concentration by volume of the zircon (28.6%), rutile (24.2%) and ilmenite (47.0%) indicates that the feedstock consists almost entirely of the VHM fraction. Trace amounts of monazite are present (< 0.2%). Grain size is variable and reflects what has been observed in the individual concentrates (Cornelius et al., 2014). The VHM concentration results are poorly supported by QEMSCAN analyses (zircon 21%; rutile 5%; ilmenite 73%) and are not considered reliable. This indicates that microCT analysis clearly require refinement when samples with multiple mineral phases are considered. The discrimination between minerals with variable chemistry and alteration products such as ilmenite and rutile for example requires attention.

6.2. Grain size

The CT images have visually shown the grain size variation between samples and also within the SCP feedstock. The results of these scans allowed the computation of grain size distributions. The method makes use of an inverted foam structure analysis, digitally separating grains and providing for each grain volume, surface area, sphericity and other quantitative values. In this work we could calculate an effective diameter of each grain based on the volume and calculating the diameter of a sphere with the same volume, referred to as the equivalent spherical diameter. An example is shown for rutile, in Fig. 10A where the CT slice image shows the grains, whilst Fig. 10B shows the colour coded analysis results for volume of each grain. The results are then presented as frequency and cumulative frequency diagrams and compared to grain size measurements as performed by the Namakwa Sands mine of the same fraction by means of grain size screening and QEMSCAN. The comparative results are graphically presented in Fig. 11 and statistical data in Table 1. The excellent correlation between the CT results and the other two methods for each mineral phase as indicated by the d_{50} for example, is clear and indicates that quantification of grain size by

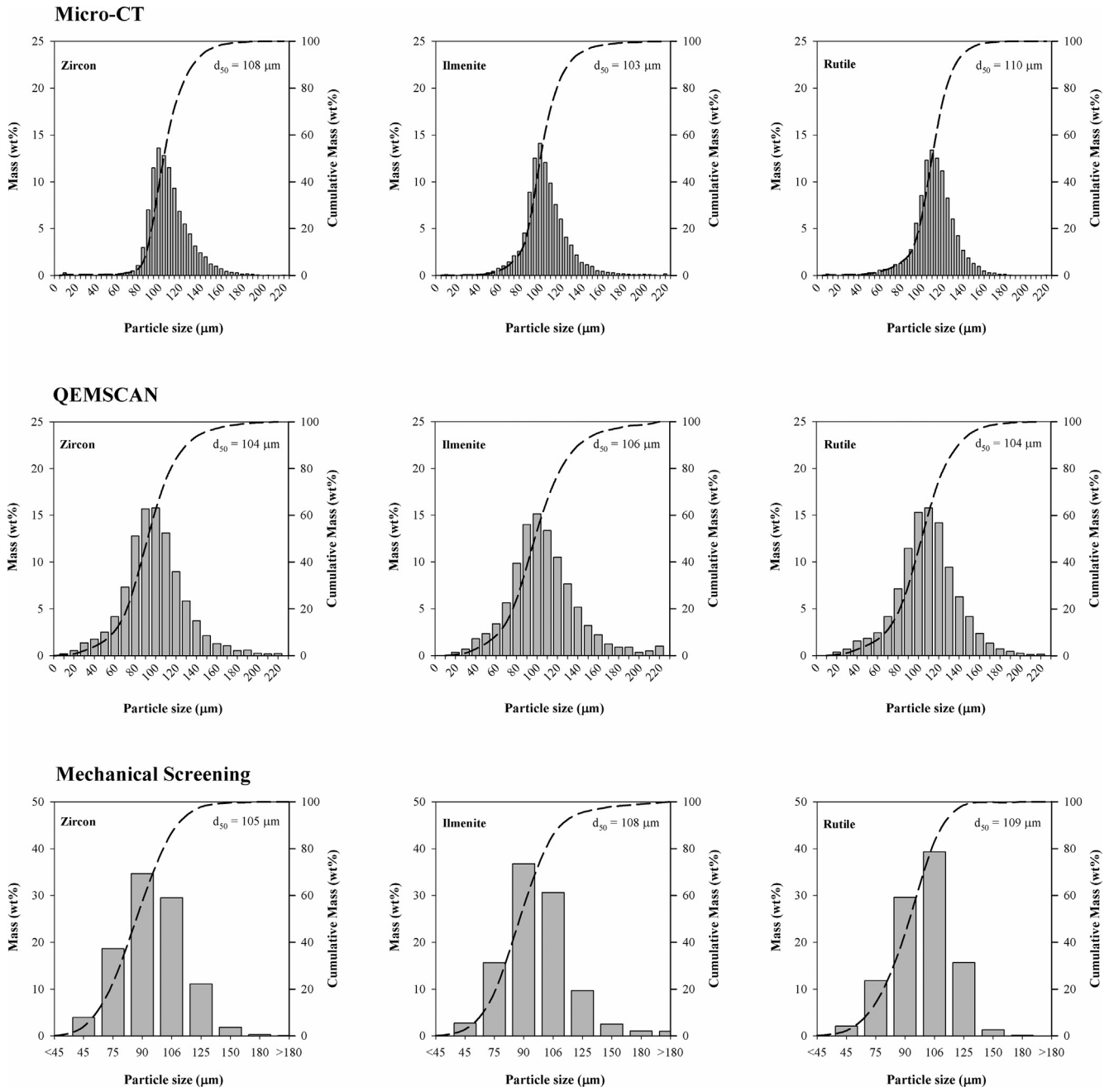

Fig. 11. Histograms showing distribution of grain size for zircon, ilmenite and rutile as determined by mechanical screening, QEMSCAN and Computed Tomography. Of the three methods, results from the microCT analyses proved to be the most realistic from a depositional environment perspective of the placer deposit.

means of microCT scanning is a feasible alternative. Grain size distribution for the various mineral concentrates shows that on average rutile is slightly coarser grained than zircon and ilmenite. This characteristic relates to its lower density and behaviour under conditions of hydraulic equivalence in fluvial and aeolian depositional environments: small dense grains behave similarly to large less dense grains under similar depositional conditions (Force, 1991). The narrow range and good correlation of grain size of the various mineral products is a result of screening the SCP feedstock between +45 and −180 µm prior to entering the MSP. Grain size is an important parameter and is a definitive characteristic of the ore body. It plays a critical role in the beneficiation process: for example a narrow range is conducive to better recovery.

Although results of the microCT analyses compare well to the other methods its grain size distribution of the three fractions is narrower than the QEMSCAN and mechanical screening methods as reflected by the steep slope of the cumulative frequency curve (Fig. 11). From a sedimentological perspective a narrow grain size distribution is an indication of high maturity of detritus normally associated with reworked aeolian and to a lesser extent marine sediments (Pettijohn et al., 1987; Force, 1991). The Namakwa Sands deposit has this particular association and it concluded that the microCT scan results are more realistic than shown by the other methods (Philander and Rozendaal, 2015a, 2015b). This can be attributed to the fact that grain size distribution by microCT scanning considers 3D images and consequently volume in its calculations thus eliminating stereological bias as imposed by 2D QEMSCAN methodology.

Grain size distribution of individual phases in the SCP feed was difficult to determine and the present method requires some development to allow this to be done with confidence.

Table 1
Results of comparative grain size study between mechanical screening, QEMSCAN and Computed Tomography. Grain size in μm.

	Statistical Parameter	Zircon	Ilmenite	Rutile
Mechanical Screening	Mean	105	108	109
	Standard Error	0.28	0.33	0.26
	Median	98	98	116
	Standard Deviation	21	25	19
	Sample Variance	441	618	377
	Kurtosis	1.89	6.17	1.35
	Skewness	0.61	1.75	0.13
	Range	209	209	209
	Minimum	23	23	23
	Maximum	231	231	231
QEMSCAN	Mean	104	106	104
	Standard Error	0.30	0.38	0.31
	Median	105	105	105
	Standard Deviation	30	38	31
	Sample Variance	922	1 453	931
	Kurtosis	1.74	4.08	3.49
	Skewness	0.48	1.24	0.53
	Range	260	280	280
	Minimum	15	15	15
	Maximum	275	295	295
Computed Tomography	Mean	108	103	110
	Standard Error	0.18	0.19	0.19
	Median	105	100	110
	Standard Deviation	20	21	19
	Sample Variance	386	452	379
	Kurtosis	3.83	4.92	4.36
	Skewness	0.61	0.97	−0.15
	Range	237	269	306
	Minimum	6	6	6
	Maximum	243	275	312

6.3. Grain shape

Variation in grain shape of the four samples is clearly visible in the images provided by the microCT scans (Figs. 5–7 and 10). Grain shape expressed as a function of sphericity was calculated for each mineral fraction by using measured surface area and volume of individual grains measured from microCT data using the described methodology. The results are presented in a series of frequency diagrams and demonstrate that in general the mineral concentrates have a similar sphericity, with zircon having a slightly higher index (Fig. 12; Table 2). The general low sphericity is the result of the primary elongated tetragonal/trigonal crystal shape of the mineral phases. The narrow range is attributed to the sediment maturity and indicates that the mineral phases have been derived from and subjected to the same sedimentological environment and depositional conditions. Sphericity range of zircon is the lowest because it is the most sedimentologically mature as indicated by its diversified provenance spanning billions of years

Table 2
Statistical parameters of sphericity histograms of the three final products.

Statistical Parameter	Zircon	Ilmenite	Rutile
Mean	0.56	0.54	0.54
Median	0.56	0.55	0.55
Standard Deviation	0.04	0.04	0.04
Sample Variance	0.00	0.00	0.00
Kurtosis	2.60	6.68	6.08
Skewness	−0.42	−1.49	−1.36
Range	0.43	0.68	0.66
Minimum	0.38	0.13	0.15
Maximum	0.81	0.81	0.81
Count	11,597	12,275	10,678

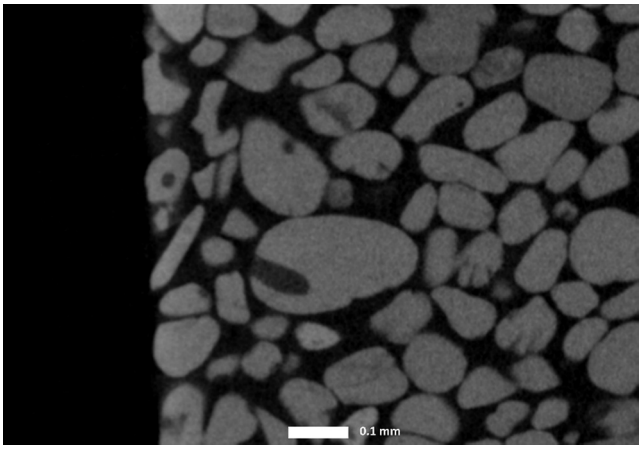

Fig. 13. Low density inclusions in ilmenite (dark grey) which could be silicate minerals reducing the quality of the final product. MicroCT voxel size 1.5 μm, field of view 1 mm.

(Philander and Rozendaal, 2015b). From a geometallurgical perspective grain shape has an influence on recovery. It has been observed that elongated grains would be more susceptible to be rejected on roll separators, on spirals and even screens. As a result sphericity indices reveal characteristics of the ore body and can be predictive in terms of expected recovery.

This type of data also allows its use in other disciplines such as sedimentology.

MicroCT scans (1.5 μm voxel size) also provided images demonstrating surface features of single grains, intergrowths and internal structures. Low density surface-connected minerals inside zircon grains were discernible (Fig. 14A). This type of impurity is a common challenge on the mine. Quantification of the percentage coverage of the grain surface should be possible. Aggregates of zircon or any other valuable heavy mineral, the result of lockings with duricrust should be

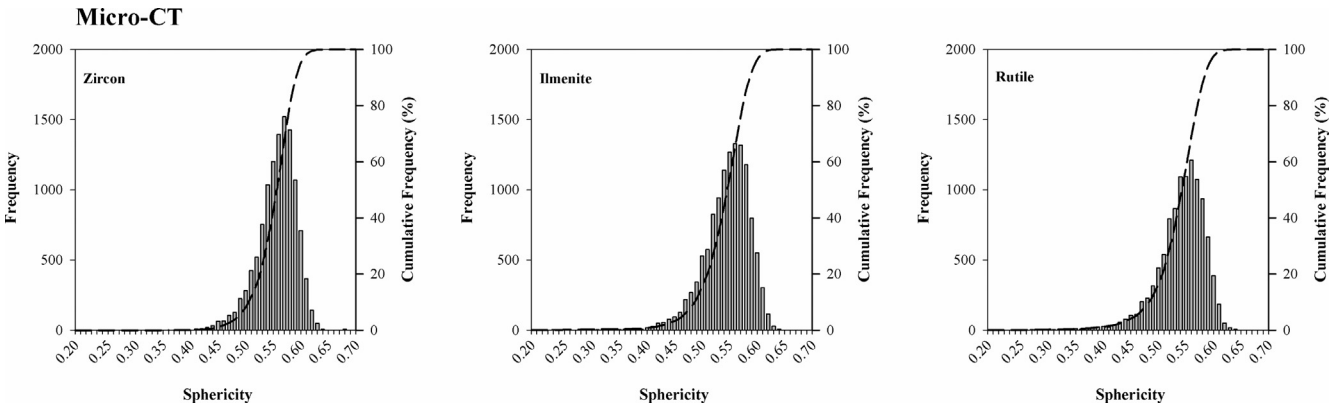

Fig. 12. Histograms showing the sphericity of the three final products.

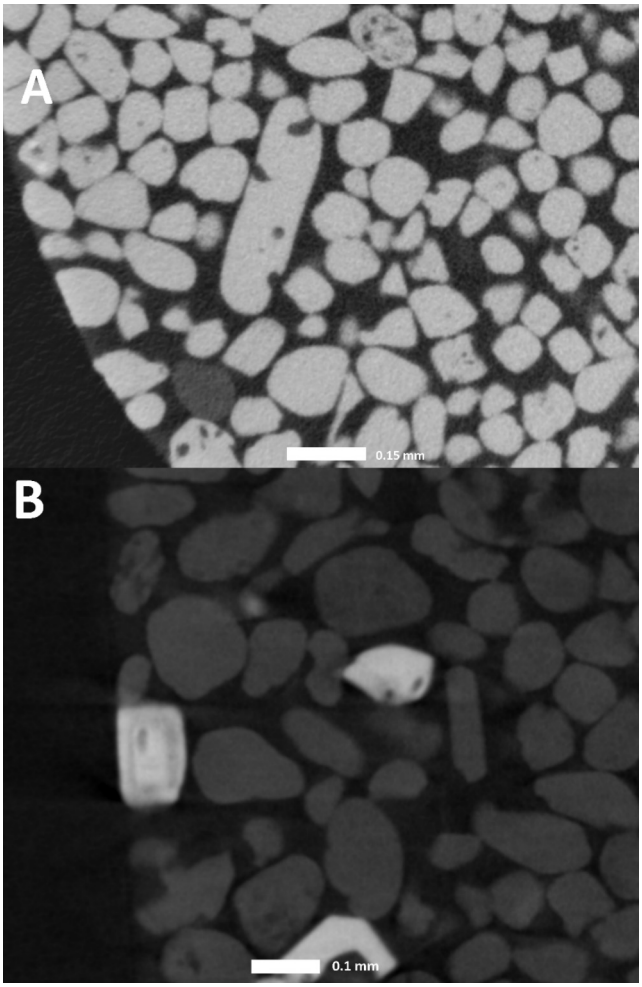

Fig. 14. Prime zircon product showing a diversity of low density internal and surface connected inclusions (A). Zircons as impurities in the prime rutile concentrate showing diagnostic concentric zoning (B). MicroCT voxel size 1.5 μm, field of view 1 mm.

clearly visible and could potentially be quantified but has not been attempted in this study. The ability to demonstrate the internal structure of complex minerals such as ilmenite can be seen in Fig. 13. Similarly are minerals such as apatite, fluid or gas inclusions in zircon or rutile visible on these scans (Fig. 14). Such data will provide an indication of deleterious impurities that are difficult to remove by mineral separation. High resolution scans show concentric zonation of high density minerals which is typical of zircon.

7. Discussion

The orientation study using four samples from the Namakwa Sands mine demonstrated that the microCT scanner has the capability to measure and quantify mineral phases and parameters that are critical in the heavy mineral industry. Individual mineral phases can be identified by using standards and concentration as volume either as gangue or ore types quantified. By converting volume to weight percent will allow the measurement of ore grade either as valuable heavy minerals (VHM) or total heavy minerals (THM), the industry standards. In addition, individual mineral concentrations can also be measured during various stages of the separation process (Fig. 3). Identification of very high density, deleterious radioactive minerals such as monazite is possible and concentration can be quantified.

Scanning results allow calculation of grain size: an important parameter particularly with respect to the in situ ore and PCP heavy mineral concentrates. The results compare well with other analytical methods such as mechanical screening or QEMSCAN of the same samples. Mineral size fraction that is recovered is set between +45 and −180 μm and grain size analyses of ROM (run-of-mine) will provide an indication of potential ore losses imposed by screening. Quantification of the latter is possible but the methodology will have to be refined in future work. Grain shape can also be determined by CT scanning and is expressed as a function of sphericity. Low sphericity elongated minerals such as zircon and rutile are often lost in the screening (classification) or other processes, resulting in a loss of VHM recovery. It is possible that this loss can be quantified.

External and internal grain characteristics are important parameters in the mineral separation process. Surface connected inclusions, particularly if mineral composition is of low density, can be identified and potentially quantified. These inclusions impair the physical characteristics of a mineral, like zircon for example, which will result in poor or non-recovery in the MSP circuit. Similarly gangue-ore aggregates can be identified and potentially quantified. Internal textural features such as intergrowths, exsolution features and alteration can be identified with high resolution scans and provide an indication of the complexity of the individual mineral grains. Abundant inclusions in zircon such as apatite for example may contribute to unwanted elements in the concentrate imposing a penalty at the sales end. Although this cannot be quantified with the microCT scans as yet, it can indicate the possible cause and guide potential solutions. At this stage the QEMSCAN and MLA analytical methods are clearly better suited to identify mineral phases and their intergrowths at high resolution, although the latter only in two dimensions. These methods presently supplement microCT studies and provide the required mineral identification used as standard reference material.

The orientation study has also highlighted the limitations of microCT at its current stage of development. Visually, in particular in 3D and qualitatively the results indicate significant potential as an analytical tool in the heavy minerals industry. Samples with relatively simple mineralogy work well and provide comparable quantitative results with other methods such as mechanical screening and QEMSCAN. Mineralogically and texturally complex samples however present a challenge and the method requires further development to bring it in line with current conventional analytical methods such as XRF geochemistry and SEM based methods which include QEMSCAN and MLA. The Namakwa Sands deposit per se offers this opportunity and further research will ensure an expanded and reliable microCT scan database for such and similar deposits. This will be required to demonstrate and develop the broad based application of the microCT scanner in the minerals industry.

8. Conclusions and recommendations

It has been demonstrated that microCT scanning technology has the potential to make a meaningful contribution to the mining and beneficiation sections of the heavy minerals industry. It has the potential to quantify several critical parameters based on 3D information and statistically meaningful database in a non-destructive one-step process. The orientation study will have to be expanded to include run-of-mine ore from both West and East ore bodies and material from the various stages in the mineral separation process to ensure representivity (Fig. 3). The results will have to be compared to those of the presently used conventional methods such as XRF, QEMSCAN, MLA and precision and accuracy demonstrated to justify its position as a supplementary and possibly alternative analytical tool in the heavy minerals industry. The viability of the method with respect to measuring and data processing time, a function of the instrument capacity should be determined and compared to the present protocol on the mine. Finally a cost-benefit analysis should be conducted to demonstrate the advantages of the new method. Provided the abovementioned outcomes are positive, development of the capacity to do real time online measurements at various stages in the mining and beneficiation process

should be considered.

The method has also demonstrated its potential application in other areas of geology such as sedimentology where quantitative data of grain size, sphericity and roundness are imperative in lithostratigraphy and basin analyses.

References

Cornelius, L.J., du Plessis, A., le Roux, S.G., Rozendaal, A., 2014. Grade determination of mineral sands using X-ray CT: proof of concept. Research report, CT Facility Stellenbosch, Stellenbosch University, p11.

Cnudde, V., Boone, M.N., 2013. High-resolution X-ray computed tomography in geosciences: a review of the current technology and applications. Earth-Sci. Rev. 123, 1–17.

du Plessis, A., le Roux, S.G., Guelpa, A., 2016. The CT Scanner facility at Stellenbosch University: an open access X-ray computed tomography laboratory. Nucl. Instrum. Methods Phys. Res., Sect. B 384, 42–49.

du Plessis, A., Broeckhoven, C., Guelpa, A., Le Roux, S.G., 2017. Laboratory X-ray micro-computed tomography: a user guideline for biological samples. GigaScience 6 (6), 1–11.

Force, E.R., 1991 Geology of titanium-mineral deposits. Spec paper 259, Geol. Soc. Am., Boulder Colorado.

Jones, G., 2009. Mineral Sands: An Overview of the Industry. Iluka Resources limited, pp. 1–26.

Ketcham, R.A., Carlson, W.D., 2001. Acquisition, optimization and interpretation of X-ray computed tomographic imagery: applications to the geosciences. Comput. Geosci. 27 (4), 381–400.

Le Roux, S.G., du Plessis, A., Rozendaal, A., 2015. The quantitative analysis of tungsten ore using X-ray microCT: case study. Comput. Geosci. 85, 75–80.

Lin, C.L., Miller, J.D., 2005. 3D characterization and analysis of particle shape using X-ray microtomography (XMT). Powder Technol. 154 (1), 61–69.

Miller, J.D., Lin, C.L., 2004. Three-dimensional analysis of particulates in mineral processing systems by cone beam X-ray microtomography. Miner. Metall. Process. 21 (3), 113–124.

Parian, M., Lamberg, P., Möckel, R., Rosenkranz, J., 2015. Analysis of mineral grades for geometallurgy: combined element-to-mineral conversion and quantitative X-ray diffraction. Miner. Eng. 82, 25–35.

Pettijohn, F.J., Potter, P.E., Siever, R., 1987. Sand and Sandstones. Springer-Verlag, New York 553p.

Philander, C., Rozendaal, A., 2014. A process mineralogy approach to geometallurgical model refinement for the Namakwa Sands heavy minerals operations, west coast of South Africa. Miner. Eng. 65, 9–16.

Philander, C., Rozendaal, A., 2015a. Geology of the Cenozoic Namakwa Sands heavy mineral deposit, west coast of South Africa: a world-class resource of titanium and zircon. Econ. Geol. 110, 1577–1623.

Philander, C., Rozendaal, A., 2015b. Detrital zircon geochemistry and U-Pb geochronology as an indicator of provenance of the Namakwa Sands heavy mineral deposit, west coast of South Africa. Sed. Geol. 328, 1–16.

Philander, C., Rozendaal, A., 2016.The geometallurgy of Namakwa Sands: challenges and solutions. In: 35th International Geological Congress, Cape Town South Africa.

Rothleitner, C., Neuschaefer-Rube, U., Illemann, J., 2016. Size and shape determination of sub-millimeter sized abrasive particles with X-ray computed tomography. In: 6th Conference on Industrial Computed Tomography (iCT), p. 2016.

Rozendaal, A., Philander, C., Heyn, R., 2017. The coastal heavy mineral sand deposits of Africa. S. Afr. J. Geol. 1 (120), 135–152.

Zhao, B., Wang, J., 2015. 3D quantitative shape analysis on form, roundness, and compactness with μCT. Powder Technol. 291, 262–275.